MODELING COMBUSTION OF STRAW-BITUMEN-PELLETS IN A FLUIDIZED BED

نموذج رياضى لإحتراق وقود بديل فى الفرن ذى المهد المميع

Okasha F.
Department of Mechanical Eng., Faculty of Engineering, Mansoura University, Egypt.
Tel. +20-12-5107427 – Fax. +20-50-2244690
Email: faroukok@mans.edu.eg

ملخص البحث

يعد الحرق المشترك مع الوقود الحفرى أسلوبا أكثر إعتمادية، وأجدى إقتصاديا لتوظيف الوقود الحيوى. وحديثا تم إقتراح وقود بديل مكون من قش الأرز والبتيومين فى صورة كريات، وذلك لإنتاج وقود اوفر طاقة، وأعلى كثافة، وأكثر إنتظاما. ويهدف هذا البحث إلى تطوير نموذج رياضى لوصف إحتراق هذا الوقود البديل فى الفرن ذى المهد المميع، حيث تم تقسيم الفرن إلى ثلاثة مناطق رئيسية وتشمل منطقة المهد المميع، ومنطقة تقاذف الحبيبات (Splashing Zone) ، والمنطقة الخالية (Freeboard zone) ، وقد تناول النموذج عددا من الظواهر الهامة، منها إنطلاق المواد الطيارة (Volatiles) واحتراقها، تفتت وتكسر الجمرات (Chars) أثناء احتراقها، تقاذف الرمل أعلى المهد، الإحتراق فيما فوق المهد، تطاير الدقائق مع الغازات.

تم حل معادلات النموذج عدديا باستخدام برناج فورتران تم بناؤه خصيصا لهذا الغرض، ومن خلال هذا البرنامج تم تحديد منحنيات التركيز للغازات، ومنحنيات توزيع درجات الحرارة وذلك على طول إرتفاع الفرن، كما تم تحديد كميات الحرارة المتولدة داخل المناطق المختلفة للفرن، كذلك تم حساب كفاءة الإحتراق ومعدلات الدقائق المتطايرة مع غازات العادم، كذلك بينت الدراسة تأثير العوامل المختلفة على أداء عمليات الإحتراق داخل الفرن.

ABSTRACT

Recently straw-bitumen-pellets have been proposed as an alternative fuel. This work presents a mathematical model for steady state combustion of straw-bitumen-pellets in a bubbling fluidized bed. The combustor is divided into three zones: dense bed, splashing zone and freeboard. Important processes including volatile segregation, char comminution and elutriation, bed particles ejection; and post-combustion in splashing zone and freeboard have been considered and simplified. Submodels for hydrodynamic, volatile release and combustion, and char consumption have been implemented. Energy balance for splashing zone and freeboard has been set to predict axial temperature profile.

Model results demonstrate that about 53% of volatiles combustion and about 62% of the total heat release take place within the bed. The fraction of heat released in the splashing zone is about 33% whereas the remainder portion (7%) releases in freeboard beyond the splashing zone. The ejected sand particles; however, recover back to the bed about 83% of heat released in the two latter zones.

The model yields the axial profiles of different species concentrations in the two bed phases (bubble and emulsion), in the splashing zone and in the freeboard. Moreover, the model predicts the axial temperature profile in the splashing and the freeboard zones that characterizes by two maxima. A small peak is built in the splashing zone with a small overheating as the ejected sand particles recover the great part of released heat. Another maximum arises in the freeboard where the flux of the ejected particles turns out to be very few and its impact on gas temperature becomes insignificant. The second maximum has relatively much higher overheating temperature.

The influences of operating variables on the combustion performance have been evaluated as well. In particular, the maximum overheating in freeboard gets higher with decreasing excess air factor, with lowering bed temperature and with increasing fluidization velocity. Bed temperature among the others has the highest impact on combustion performance.

An acceptable agreement are found between the predicted and the measured concentrations and temperature profiles.

Keywords: Modeling, Fluidized bed, Co-combustion, Biomass, Bitumen, Alternative fuel

Accepted June 29, 2006

NOMENCLATURE

A_{bed} bed cross section area, m^2
A_{sp} cross section area of splashing zone, m^2
Ar_s Archimedes number for bed materials
C molar concentration, kmole/m^3
$C_{ej,s}$ exponential decay constant, m^{-1}
Cp_g specific heat capacity of gases, J/(kg.K)
Cp_s specific heat capacity of sand, J/(kg.K)
d_{ch} average diameter of char, m
$d_{ch,o}$ initial average size of fed fuel pellets, m
d_s average size of bed particles, m
EA Excess air factor, dimensionless
g acceleration of gravity, m/s^2
$h_{w,ov}$ overall heat transfer coefficient through the combustor wall, J/(m^2.s.K)
$h_{ej,s}$ heat transfer coefficient to an ejected sand particle, J/(m^2.s.K)
H_{eb} expanded bed height, m
H_{mf} bed height at minimum fluidization, m
HR heat of reaction, J/kmole
K_{be} coefficient of mass interchange between bubble and emulsion phase, s^{-1}
k_{ch} reaction rate constant for char combustion, m/s
k_{CHy} reaction rate constant of hydrocarbon, $m^{1.5}/(kmole^{0.5}.s)$
k_{CO} reaction rate constant of carbon monoxide, m^3/(kmole.s)
k_m mass transfer coefficient, m/s
L_{sp} peripheral of the combustor cross-section in the splashing zone, m
M molecular weight, kg/kmole
M_s mass flux of ejected sand, kg/(m^2.s)
M_{so} initial mass flux of ejected sand particles, at the surface, kg/(m^2.s)
$\dot{m}_f$ mass rate of fuel feed into the bed, kg/s
n_1 particle multiplication factor due to primary fragmentation
n_2 particle multiplication factor due to secondary fragmentation
Ng molar flow rate of gases, kmole/s
q_i local rate of species release, kmole/(s.m)
Q_i cumulative rate of species release, kmole/s
$\bar{Q}_i$ species release rate from fuel, kmole/s
Q_s local heat transfer rate between ejected sand and gases, J/(s.m)
Q_w local heat transfer through wall, J/(s.m)
$\dot{r}_{ch,g}$ specific carbon combustion rate at char surface, kg/(m^2.s)
$R_{ch,g}$ char combustion rate, kg/s
$R_{ch,fine}$ fine generation rate from coarse char, kg/s
R reaction rate, kmole/(m^3.s)
R_{CHy} reaction rate of CH_y, kmole/(m^3.s)
R_{CO} reaction rate of carbon monoxide, kmole/(m^3.s)
R_μ universal gas constant, J/(kmole.K)
T temperature, K
T_{am} ambient temperature, K
T_{bed} bed temperature, K
T_{ch} char temperature, K
T_s temperature of ejected sand particles, K
$T_{g,sp}$ gas temperature in splashing zone, K
t time, s
u_b bubble rise velocity, m/s
u_e superficial velocity of the gas through the emulsion phase, m/s
u_{mf} superficial gas velocity at minimum fluidization conditions, m/s
u superficial gas velocity, m/s
u_{sp} superficial gas velocity in splashing zone, m/s
V_{ash} volume fraction of ash in char particle
W_{ch} load of char in the bed, kg
x mass fraction of constituent in fuel
y molar hydrogen fraction in the hydrocarbon due to devolatilization,
z height above gas distributor, m

Greek Symbols

α coefficient in Eq. 18, dimensionless
α_{v1} fitting factor for CHy oxidation
α_{v2} fitting factor for CO oxidation
β constant in equation 3
ε_{mf} voidage fraction in the emulsion phase at minimum fluidization
θ_{cr} char initial porosity, dimensionless

θ_o char critical porosity, dimensionless
ρ_{ch} char density, kg/m^3
ρ_s density of bed particles, kg/m^3
δ fraction of bed in bubble

Subscripts
b bubble
ch char
e emulsion
eb expanded bed
ej ejected
F fuel
FC fixed carbon
g gases
mf minimum fluidization
o initial
ov overall
s sand particle
sp splashing
w wall

1. INTRODUCTION

Utilization of biomass energy has growing interest for reducing greenhouse effect as well as lessening the dependence on fossil fuels. In many cases; however, there are some difficulties including cost, availability and/or quality that limit the use of biomass. The co-combustion with fossil fuel seems to be a more concrete option to overcome those difficulties and to expand economically utilization of biomass fuel (Ekmann et al., 1996; and Adanez et al., 2003). Several studies have dealt with the co-combustion of biomass and coals (Leckner and Karlsson, 1993; Hein and Bemtgen, 1998; Armesto et al., 1997; Fahlstedt, 1997; Werther et al., 2000; Karakas, 2001; and Amand et al., 2001).

Recently co-combustion of biomass and bitumen has been performed by Okasha et al. (2006). The authors proposed an alternative fuel that consists of rice straw and bitumen pellets. Experiments showed that pellets of rice straw and bitumen are attractive to be used as an alternative fuel being characterized by a relatively high combustion efficiency, moderate NO_x emissions (peak value= 128-135 ppm) and "intrinsic" sorbent capability plied by ashes of rice straw.

The combined biomass-bitumen fuel like many other alternative fuels has physical and chemical characteristics much different from coal that greatly affect the combustion performance. The lower density affects the fuel distribution inside the combustor. The higher volatile content calls attention to mixing/segregation phenomenon. Yates et al. (1980), Atimtay (1980), Pillai (1981) and Fiorentino et al. (1997a, b) observed bubbles formation around devalatilizing fuel particles. The draft effect of forming bubbles in addition to the lower density of biomass causes segregating fuel particles near the bed surface (Davidson 1992). Furthermore, the friable structure of remaining char has a major impact on the comminution phenomena. As reported by Gulyurtlu et al. (1984 and 1991), Arena et al. (1995a, 1995b and 1996), Salatino et al. (1997 and 1998) and Scala et al. (2000), the generated carbon fines due to fragmentation and attrition are much greater compared with that of coal. Therefore, the combustion modeling of those alternative fuels needs reconsideration for most of fundamental processes.

In pioneer modeling work on fluidized bed combustion of high volatiles solid and liquid fuels a diffusion-based plume model was proposed by Park et al. (1980 and 1981) and Stubington and Davidson (1981). Stubington et al. (1990 and 1993) suggested a multiple discrete diffusion flame model which accounts for devolatilizing particles stepwise motion to the top of the bed under the action of the ascending fluidizing gas bubbles. A three-phase FBC model has been proposed by Irusta et al. (1995) that took into consideration comminution phenomena. Volatile was assumed to release partially in the bed and partially in the freeboard based on an adjustable parameter. Borodulya et al. (1995) presented a modified two-phase

plume model for fluidized bed combustion of biomass. The model takes into account combustion of volatile and chars in the bed as well as the freeboard in which about 40% of volatile burns according the model prediction. A comprehensive model for continuous combustion of lignite in an atmospheric bubbling fluidized bed is presented by Selcuk et al. (2001). In the latter work the model of Stubington et al. (1990) is applied to estimate the fractions of volatiles released within the bed and in the freeboard. Volatiles are assumed to be released uniformly in the emulsion phase. The model estimates that about 9% of volatiles are released in the freeboard considering bottom feeding of lignite particles. More recently Scala and Salatino (2002) proposed a model for fluidized bed combustion of high volatile solid fuels. The model takes into account phenomena that assume particular importance with high-volatile solid fuels, namely fuel particle fragmentation and attrition, volatile matter segregation and post-combustion above the bed. The model calculations indicate that combustion occurs to comparable extents in the bed and in the splashing region of the combustor. Extensive bed solids re-circulation associated to solids ejection/falling back due to bubbles bursting at bed surface promotes thermal feedback from this region to the bed of as much as 80–90% of the heat released by afterburning of volatile matter and elutriated fines.

Miccio et al. (2001), Faravelli et al. (2003 and 2004) and Scala et al. (2004) have given a significant contribution for modeling of combustion of liquid in FB. The modeling development has been centered on the fate of rising fuel vapor bubble as a consequence of reaction, mass and heat transfer. A simplified model for desulphurization of heavy liquid fuel has been proposed by Miccio and Okasha (2004). Okasha and Miccio (2006) have developed a model for the interaction of the assisted-air-liquid fuel jet with fluidized bed particles. The model can predict the rate of liquid fuel evaporation inside the jet flare. Moreover, the model can be utilized to determine the initial concentrations of fuel vapor in bubble and emulsion phases. More recently a one-dimensional model for continuous combustion of liquid fuels in fluidized beds has been presented by Okasha (2006).

In this paper a model for fluidized bed combustion of straw-bitumen-pellets has been developed. The model considers the important aspects discussed above including volatile release and segregation, char combustion and comminution; and post-combustion in the splashing and the freeboard zones. The model yields the concentration profiles of different species in the two phases of the bed, in the splashing zone and in the freeboard. In particular the model is able to predict the temperature profile within the splashing and the freeboard zones.

2. MATHEMATICAL MODEL

A one dimensional model for fluidized bed combustion of straw-bitumen-pellets is developed and described. The combustor is axially divided in three zones: dense bed, splashing zone and freeboard. The gases in the three zones including the emulsion phase are assumed in plug flow. The conservation equations of chemical species are expressed in the three zones. Five chemical species (CH_y, O_2, CO, H_2O and CO_2) are considered in this model. Energy equations of the splashing zone and the freeboard are derived to predict axial temperature profile.

2.1. Hydrodynamic

The bed is modeled according to the two-phase theory of fluidization (Toomey & Johnstone 1952; Davidson & Harrison 1963). As recognized by Hilligardt and Werther (1986) and Kunii and Levenspiel(1991) the superficial gas velocity through the emulsion u_e is given by the following expression instead of minimum fluidization velocity u_{mf}.

$$(u_e - u_{mf})/(u-u_{mf}) = 1/3 \quad (1)$$

The excess of gas $(u_o - u_e)$ passes through the bed as bubbles. An average bubble size is assumed and estimated according to Darton et al. (1977). Bubbles are assumed to be solids free. The gases in both bubble and emulsion phases are assumed to be in plug flow. The mass transfer between the emulsion phase and the bubble phase is determined using the correlations reported by Kunii and Levenspiel (1991).

The splashing zone is located above the bed zone where a more effective mixing is established due to bubbles erupting (Pemberton and Davidson, 1984; and Van der Honing, 1991). The gas is assumed to be in plug flow after instantaneous mixing at the bed surface. Ejected bed particles and elutriated fines are in uniform distribution neglecting clustering of particles as suggested by Benoni et al. (1994). The mass flux of ejected sand particles is expressed with the following exponential decay function.

$$M_s = M_{so} \exp[-C_{ej,s}(z - H_{eb})] \quad (2)$$

where M_{so} is the initial mass flux at the bed surface and may be given by (George and Grace 1978; Pemberton and Davidson 1986)

$$\dot{M}_{so} = \beta.\rho_s(1-\varepsilon_{mf})(u_o - u_{mf}) \quad (3)$$

In the present work the parameter β is assumed to be 0.1 although the proposed values in literatures have a broad range (George and Grace, 1978; Pemberton and Davidson, 1986; Briens et al., 1988; Baron et al., 1990; Fung and Hamdullahpur, 1993; and Milioli and Foster, 1995). $C_{ej,s}$ is an adjustable parameter and H_{eb} is the expanded bed height.

2.2. Volatile Release and Combustion

Previous studies (Prins, 1987; Madrali et al., 1991; Ogada, 1995 and Fiorentino et al., 1997a b) indicated that the fuel particles tend to concentrate close to the bed surface during devolatilization period. This consequence may be attributed to the draft effect of forming volatiles bubbles (Davidson 1992). This is particularly true with biomass fuel because of the higher volatile content and the lower density. The formation of bubbles around devolatilizing fuel particles is observed by many authors (Yates et al., 1980; Atimtay, 1980; Pillai, 1981 and Fiorentino et al., 1997a,b). According to Fiorentino et al. (1997a,b) the released volatiles tend to form bubbles whereas the amount of volatile that percolates through the emulsion phase is very small less than 1%.

It is more probably that those embryonic bubbles forming due to volatile release are engulfed by the larger bubbles formed at the air distributor and grew along the bed height. Accordingly, as a first approximation the volatiles are assumed to release in the bubble phase according to a distribution function of the bed height, z.

$$q_i = \frac{dQ_i}{dz} = \frac{4\overline{Q}_i}{H_{eb}^4} z^3 \quad (4)$$

This function form is an adjustable parameter chosen based on experimental results as discussed below. $\overline{Q}_i$ is the feeding molar rate of moisture and volatile species that may be calculated as:

$$\overline{Q}_{H_2O} = \dot{m}_F.x_{H_2O}/M_{H_2O} \quad (5)$$

$$\overline{Q}_{O_2} = \dot{m}_F.x_O/M_{O_2} \quad (6)$$

$$\overline{Q}_{CH_y} = \dot{m}_F(x_C - x_{FC})/M_C \quad (7)$$

In this stage sulfur and nitrogen aren't considered. The volatile is assumed to release as hydrocarbon CH_y (Philippek et al. 1997). The value of y can be calculated from the ultimate analysis.

$$y = \frac{x_H.M_C}{(x_C - x_{FC}).M_H} \quad (8)$$

Two-step reaction is applied for volatile combustion. Volatile primarily reacts to carbon monoxide and water vapor. The rate

of hydrocarbon conversion is determined by an expression developed by Dryer and Glassman (1973).

$$R_{CH_y} = -k_{CHy}[C_{O_2}]^{0.8}[C_{CH_y}]^{0.7} \quad (9)$$

with

$$k_{CHy} = \alpha_{v1} 1.58*10^{10}.\exp[-24157/T] \quad (10)$$

α_{v1} is a fitting factor for higher oxygen concentration that was experimentally determined by Philippek et al. (1997) to be 30.

In the second step carbon monoxide reacts with oxygen to form carbon dioxide. The expression developed by Howard et al. (1973) is used to calculate the rate of the latter reaction.

$$R_{CO} = -k_{CO}.C_{CO}.(C_{H2O}.C_{O2})^{1/2} \quad (11)$$

where

$$k_{CO} = \alpha_{v2}.1.3.10^{11}.\exp[-15088/T] \quad (12)$$

According to Hayurst and Tucker (1990) the large surface of solid particle in fluidized bed deactivates radicals leading to a reduction in CO oxidation rate. The results obtained by Loeffler and Hofbauer confirmed that oxidation rates are significantly reduced in the particulate phase whereas the effect of heterogeneous radical quenching is slight in the bubble phase. The factor α_{v2} is inserted to take into consideration the impact of radical quenching. α_{v2} is considered 1.0 in bubble phase and is taken to be 0.1 as experimentally determined by Philippek et al. (1997).

2.3. Char Consumption

Char inside the bed is consumed by combustion process and due to comminution impacts. The char burning is described by a shrinking particle model assuming CO_2 as the dominant product (Leckner et al., 1992 & Adanez et al., 2001). Taking diffusion and kinetic resistances into consideration and assuming a first order reaction with respect to oxygen, the specific rate of carbon conversion at the char surface may be given as

$$\dot{r}_{ch,g} = \frac{-12C_{O_2}}{(1/k_m + 1/k_{ch})} \quad (13)$$

where mass transfer coefficient k_m is calculated using an empirical correlation proposed by Leckner et al. (1992). Kinetic of char combustion k_{ch} is estimated by an expression obtained by Adanez et al (2001). However; the coefficients of the equation are slightly modified to fit better with experimental results of batch combustion tests performed on rice straw-bitumen-pellets (Okasha et al., 2006).

$$k_{ch} = 1.045 * T_{ch} \exp(-70400/R_\mu.T_{ch}) \quad (14)$$

The char temperature is assumed to be uniform and is calculated by the following correlation (Leckner et al., 1992 and Borodulya et al., 1995).

$$T_{ch}/T_{bed} = 0.84 Ar_s^{0.05} \quad (15)$$

The combustion rate of char particles with a load, W_{ch}, is evaluated using the equation:

$$R_{ch,g} = \frac{6W_{ch}}{\rho_{ch}.d_{ch}} \dot{r}_{ch,g} \quad (16)$$

where ρ_{ch} is the char density and d_{ch} is the average diameter of the char particle in the bed that is expressed according to Chirone et al. (1984) and Arena et al. (1995)

$$d_{ch} = 0.8 d_{ch,o}[n_1(\frac{n_2+1}{2})]^{-1/3} \quad (17)$$

where n_1 and n_2 represent the char particle multiplication factors due to primary and secondary fragmentations, respectively.

The burning char particle yields fines due to fragmentation by peripheral percolation and surface abrasion. For the high volatile biomass fuel fines generation is proportional to the carbon-burning rate at the particle surface. The fine generation rate may be expressed as (Salatino et al., 1998; and Scala and Salatino, 2002)

$$R_{ch,fine} = -\alpha . R_{ch,g} \quad (18)$$

where

$$\alpha = (\frac{1 - V_{ash} - \theta_{cr}}{\theta_{cr} - \theta_o}) \quad (19)$$

θ_o and θ_{cr} are the char initial and critical porosities, respectively, and V_{ash} is the volume fraction of ash in the char particle. Equation 16 is also used for fine char combustion rate. The average diameter of fine char is assumed to be constant (Arena et al., 1983) and may be taken 100 μm for biomass fuels as suggested by Chirone et al. (1999)

2.4. Mass and Energy Balance Equations

2.4.1. Bed zone

The bed is considered isothermal where the two phases have a uniform temperature, namely, bed temperature. Five species have been treated that include released volatile as hydrocarbon (CH_y), oxygen (O_2), water vapor (H_2O), carbon monoxide (CO) and carbon dioxide (CO_2). Axial variation of the species concentrations may be described by the following differential equations.

Mass balance of species i in bubble phase b

$$\frac{dC_{b,i}}{dz} = \frac{K_{be}}{u_b}(C_{e,i} - C_{b,i}) + \frac{1}{u_b}(\sum R_{b,i}) + \frac{1}{A_{bed}.\delta.u_b} q_i \quad (20)$$

Mass balance of species i in emulsion phase e

$$\frac{dC_{e,i}}{dz} = \frac{K_{be}.\delta}{u_e}(C_{b,i} - C_{e,i}) + \frac{\varepsilon_{mf}(1-\delta)}{u_e}(\sum R_{e,i}) \quad (21)$$

In the latter equations the first term of the right hand side represents the exchange of gases between emulsion phase and bubble phases. The second term accounts for the sum of generation and consumption of i^{th} component due to chemical reaction. Those latter take the following expressions:

Hydrocarbon (CH_y) i=1

$$\sum R_{b,1} = R_{CHy,b} \quad (22)$$

$$\sum R_{e,1} = R_{CHy,e} \quad (23)$$

Carbon monoxide (CO) i=2

$$\sum R_{b,2} = -R_{CHy,b} + R_{CO,b} \quad (24)$$

$$\sum R_{e,2} = -R_{CHy,e} + R_{CO,e} \quad (25)$$

Carbon Dioxide (CO_2) i=3

$$\sum R_{b,3} = -R_{CO,b} \quad (26)$$

$$\sum R_{3,e} = -R_{CO,e} - \frac{R_{ch,g}}{12} - \frac{R_{fine,g}}{12} \quad (27)$$

Water vapor (H_2O) i=4

$$\sum R_{b,4} = -(y/2).R_{CHy,b} \quad (28)$$

$$\sum R_{e,4} = -(y/2).R_{CHy,e} \quad (29)$$

Oxygen (O_2) i=5

$$\sum R_{b,5} = 0.5(1 + \frac{y}{2})R_{CHy,b} + 0.5R_{CO,b} \quad (30)$$

$$\sum R_{e,5} = 0.5(1 + y/2).R_{CH,e} + 0.5R_{CO,e} + R_{ch,g}/12 + R_{fine,g}/12 \quad (31)$$

The mass balance on the coarse char is given as

$$\dot{m}_{fc} = -R_{ch,g} - R_{ch,fine} \quad (32)$$

2.4.2. Splashing Zone

Mass balance of species, i, in splashing zone, sp, is expressed as

$$\frac{dC_{sp,i}}{dz} = \frac{1}{u_{sp,g}}(\sum R_{sp,i}) \quad (33)$$

The terms $R_{sp,i}$ have expressions similar to those of emulsion phase but with dropping coarse char items where the splashing zone is assumed to be coarse char free.

4.1. Base Case Measurements and Computations

Steady state combustion experiments have been carried out to determine the two adjustable parameters of the model, namely, the distribution function of volatile release and the exponential decay constant for ejected sand particles. A comparison between measurements and predicted results is also done to assess the validity of the proposed model. The experiments have been conducted under the base case conditions. The superficial gas velocity was adjusted to 1.0 m/s and the bed temperature was maintained at about 850 °C while the excess air factor was kept at 1.2. Sand of a 0.65 mm mean size was considered for the base case. The used fuel pellets have a diameter of 15 mm and a length of 15 mm.

The axial profiles of species concentrations and temperature have been estimated using the model considering the base case conditions. The obtained results are presented in Fig.s 1-6.

The predicted profiles of hydrocarbon are shown in figure 1. Clearly CH_y concentration grows much faster in bubble phase as volatiles species are assumed to be released only in bubble phase. The rate of increment is small in the lower part of the bed whereas it multiplies with height in accordance with equation 5. Existence of hydrocarbon in emulsion phase is on account of mass transfer process. The concentrations of CH_y reach maximums at the bed surface while the volatile release brings to an end. It is interesting to state that about 53% of volatiles complete burning in the bed according the model estimation under the base case conditions (see table 2). This value is comparable with that estimated by Borodulya et al. (1995) which is about 60%.

Oxygen concentration reduces faster in emulsion phase as shown in figure 2. This should be ascribed to char combustion that is assumed to be uniformly fed in emulsion phase. However, the oxygen concentration in bubble phase turns out to be lower in the upper part of the bed as the hydrocarbon oxidation becomes more intensive.

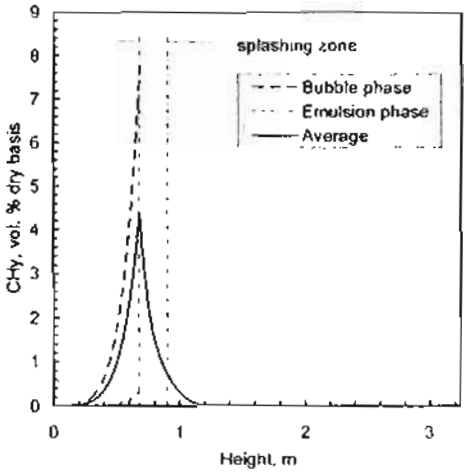

Fig. 1. Profiles of hydrocarbon concentration at the base case conditions

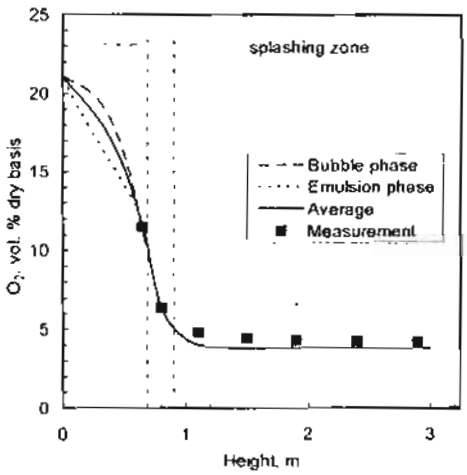

Fig. 2. Profiles of oxygen concentration at the base case conditions

The higher oxidation rate of hydrocarbon in bubble phase results in a higher H_2O concentration as shown in figure 3. Of course the increment in H_2O concentration is partly attributed to releasing fuel moisture content in bubble phase as well. The divergence between the profiles of H_2O concentration considerably grows with height as the release of volatiles and moisture contents multiplies. On the contrary, CO concentration profiles presented in figure 4 exhibit a convergence with bed height. This trend should be ascribed to the higher oxidation rate of carbon monoxide in bubble phase. On the

other side, the oxidation rate of CO in emulsion phase is very slow mainly for three reasons: deactivation of radicals by solid particle, the lower concentration of H_2O (See Eq. 11 and Fig. 3) and the lower concentration of O_2 (See Eq. 11 and Fig. 2).

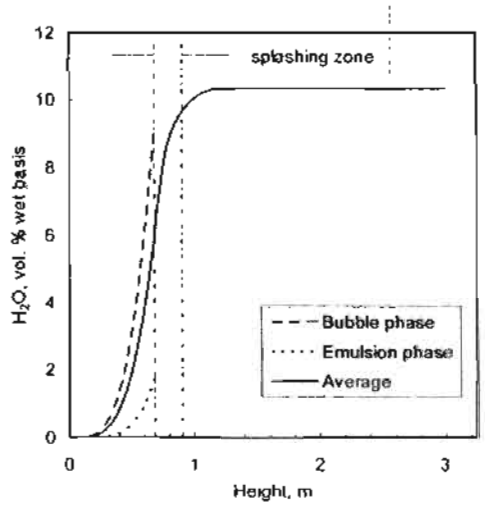

Fig. 3. Profiles of water vapor concentration at the base case conditions

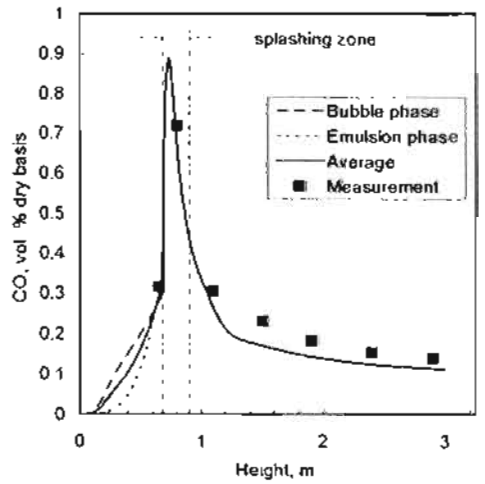

Fig. 4. Profiles of carbon monoxide concentration at the base case conditions

The axial concentration profiles of carbon dioxide are presented in Fig. 5. CO_2 concentration in emulsion has approximately a linear trend that mainly demonstrates the uniform burning of char in emulsion phase. On the other side, CO_2 concentration profile in bubble phase is in accordance with the volatile release function (see Eq. 4).

In the splashing zone the concentration profiles exhibit very fast changes as the species of the two phases are assumed to be instantaneously well mixed at the bed surface. As shown in figures 1 and 4 CH_y concentration rapidly drops while CO profile has an acute peak. There are also major changes in the concentrations of O_2, H_2O, and CO_2 as shown in figures 2, 3 and 5, respectively.

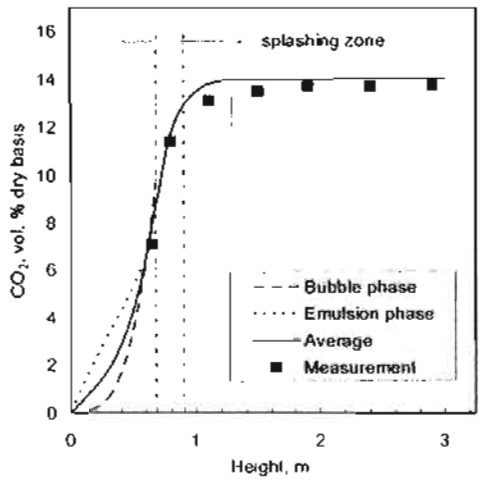

Fig. 5. Profiles of carbon dioxide concentration at the base case conditions

Figure 1 also illustrates that a non-negligible portion of hydrocarbon still completes burning in the freeboard beyond the splashing zone. CH_y concentration; however, reduces close to zero at height of 1.25 m above the distributor. On the other side, carbon monoxide concentration steadily diminishes along the freeboard height.

The measured values of O_2, CO and CO_2 concentrations are also plotted in figures 2, 4 and 5, respectively. A good agreement between the measurements and the predicted profiles is observed.

The predicted axial temperature profile is shown in figure 6 in comparison with measured values considering the base case conditions. The model results are in an acceptable agreement with the measurements.

The predicted temperature profile yields a small peak in splashing zone with a maximum temperature of 10 °C overheating. The overheating appears relatively very small as the intensive combustion reactions in this zone release about 33% of the total

heat. The ejected sands particles; however, recover the great part of the released heat that damps the overheating for higher temperature. In fact, the model calculations estimate that 83.3% of heat released above the bed zone is recovered by the ejected sand particles (see table 2). This latter value is well comparable with that obtained by Scala and Salatino (200) where they estimated the recovered heat to be 80-90%. Past the splashing zone gas temperature begins to increase with higher rates and the profile exhibits another peak. This latter peak has a much higher overheating, about 66 °C above the bed temperature even though the fraction of heat released in this zone doesn't exceed 7%. Certainly the ejected sand particles that travel beyond the splashing zone turn out to be very few. Thereby the heat recovered by them is negligible and its impact on gas temperature becomes insignificant. This latter finding has been experimentally confirmed by Miccio et al. (2003) where the maximum gas temperature was found above the splashing zone. The phenomenon of overheating of gas in freeboard has been experimentally confirmed by many authors (Peel & Santos, 1980; Hampartsoumian and Gibbs, 1980; Gulyurtlu and Cabrita, 1984; Achara et al., 1984; Jovanovic and Oka, 1984; Leckner et al., 1984; Andersson et al., 1985; and Irusta et al., 1995). After the maximum point the gas temperature gradually decreases due to the heat loss through the combustor wall.

The concentrations of coarse and fine chars in the bed are presented in figure 7 as a function of height. The char concentration increases with height as the oxygen concentration in emulsion phase gradually lessens (see in figure 2). The char concentration close to the bed surface is about twofold of that near the distributor. This trend is based on the assumption that original char of the fed fuel is uniformly distributed along the bed height. The latter results appear more realistic than the assumption of uniform char concentration as many authors experimentally found that the biomass char tends to be more concentrated close to bed surface (Miccio et al., 2003; Philippek et al., 1997 and Ogada, 1995). Certainly the finer char has much lower concentration since it has much larger burning rate owing to the very much larger surface area. The average concentrations of coarse and fine char in bed are reported in table 2. The table also reports the fractions of elutriated carbon at the bed surface and at the combustor exit. The elutriated carbon is very small and fixed carbon burning efficiency is close to unity although a large amount of elutriable fines is generated due to percolative fragmentation. It appears that the high reactivity allows fast burning of fine chars during their residence in the bed. These results are in accordance with that obtained by Scala and Salatino (2002).

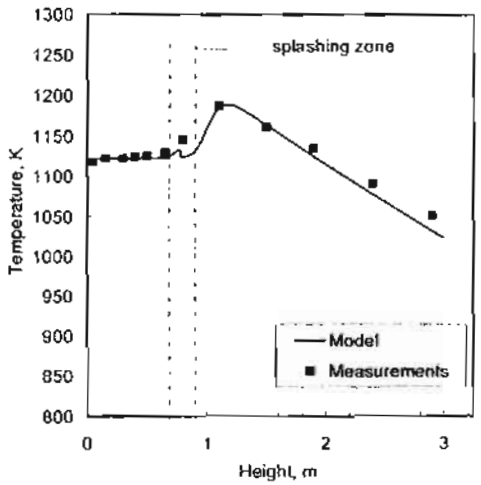

Figure 6. Axial temperature profile at the base case conditions

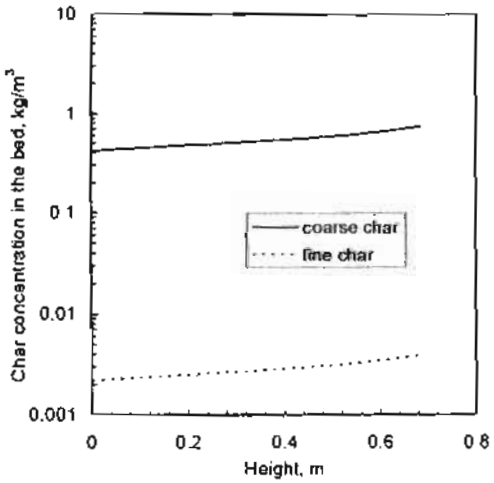

Fig. 7. Axial char concentration in the bed at the base case conditions

Combustion efficiency on energy basis is reported in table 2 as well. The predicted combustion efficiency is very high, near complete combustion is obtained.

For the applied fuel, the initial and critical porosity (θ_o and θ_{cr}) aren't well-known. Alternatively, the corresponding values for robina reported by Scala and Salatino (2002) have been used to calculate the coefficient α using equation 19. Therefore, a sensitivity analysis has been performed to assess the impact of the coefficient α on the model outputs and the obtained results have been reported in table 2. The results indicate that the deviation in coefficient α has a moderate impact only on the char concentrations and elutriated fixed carbon. On the other hand, it has insignificant effects on the other outputs including species concentrations and temperature profiles; and combustion efficiency.

Tab. 2. Model results and sensitivity analysis at the base case conditions

		base case		Sensitivity
Coefficient in Eq. 18, α	0.75	0.965	0.98	
Fraction of volatile burned within the bed, %	52.87	52.87	52.87	≈ 0.0
Fraction of heat release within the bed, %	61.77	61.77	61.77	≈ 0.0
Fraction of heat recovered by ejected sand, %	83.3	83.3	83.3	≈ 0.0
Average concentration of coarse char in the bed, kg/m^3	0.593	0.535	0.530	0.513
Average concentration of fine char in the bed, kg/m^3	.00250	0.00282	0.00285	0.514
Ratio of elutriated FC from the bed to fed FC	3.35e-4	3.78e-4	3.82e-4	0.513
Maximum temperature in freeboard, K	1189	1189	1189	0
Maximum overheating above bed temperature, °C	66	66	66	0
Maximum CH_y concentration, %	4.11	4.11	4.11	0
Maximum CO concentration, %	0.823	0.823	0.823	0
Exhausted CO concentration, %	0.102	0.102	0.102	0
Ratio of exhausted FC from the combustor to fed FC	1.7e-6	1.92e-6	1.94e-6	0.514
Combustion efficiency, %	99.59	99.59	99.59	5.09e-7

4.2. Influence of Operating Variables

The influences of the most important operating variables on the combustion performance have been estimated and discussed below. The studied variables include excess air factor, bed temperature and fluidization velocity.

4.2.1. Influence of excess air factor

The mathematical model has been used to predict the influence of excess air factor on combustion performance while keeping all other variables at the base case conditions. The obtained results are presented in Fig.s 8 and 9 as well as table 3.

The axial profile of CH_y concentration is shown in figure 9.a as a function of excess air factor. The peak becomes more pronounced with decreasing excess air factor while the maximum value of CH_y concentration turns to be greater as reported in table 3. The result appears reasonable as CH_y oxidation rate reduces at a smaller value of excess air factor due to the lower concentration of O_2 (see figure 9.c and Eq. 9). The results imply that a higher fraction of unburned hydrocarbon reaches splashing zone at a smaller excess air factor as indirectly reported in table 3. Accordingly, the pos-combustion of CH_y in splashing zone becomes more intensive resulting in a higher concentration of carbon monoxide. The latter consequence is demonstrated in figure 8.b and in table 3 where the peak of CO profile develops into higher and the maximum value becomes greater. Figures 8.a and 8.b also illustrate that larger fractions of CH_y and CO burn in the freeboard above the splashing zone with decreasing excess air factor.

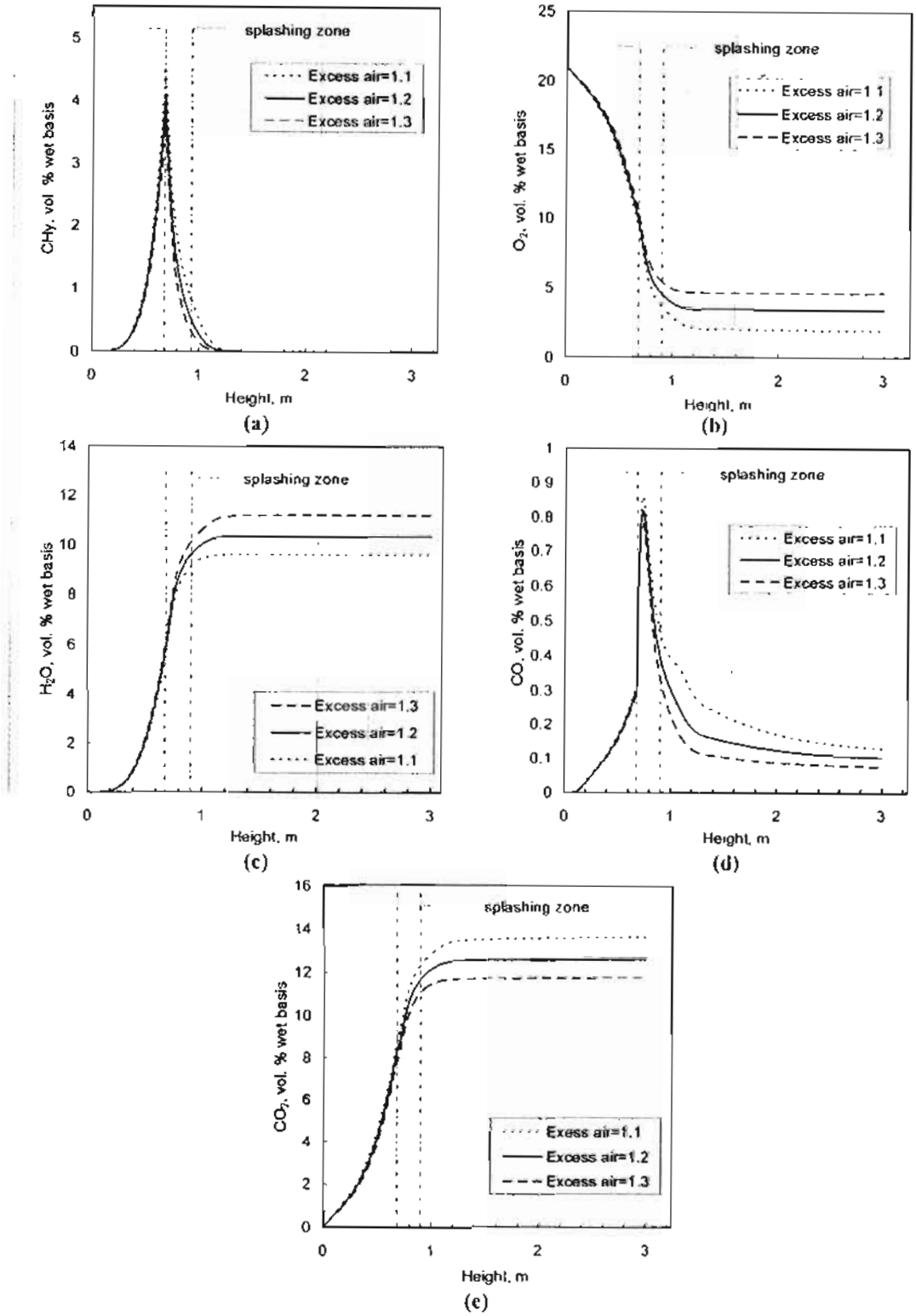

Fig. 8. Influence of excess air factor on species concentration profiles

The axial profile of gas temperature as a function of excess air factor is shown in figure 9. The gas temperatures are practically the same in the splashing zone whatever the excess air factor. It appears that the ejected sand particles have the ability to damp the gas temperature regardless the fraction of heat released in the plashing zone. Alternatively, beyond the splashing zone the gas temperature becomes

higher with decreasing excess air factor. The maximum gas temperatures are estimated to be 1236 1189 and 1161 K with overheating above the bed temperature 113, 66 and 38 °C for excess air factor 1.1, 1.2 and 1.3, respectively (see also table 3). In fact beyond the splashing zone the flux of ejected sand particles turns out to be very low and the heat recovered by those particles becomes insignificant. Therefore, the rates of heat released due to burning processes are directly demonstrated as gas temperatures.

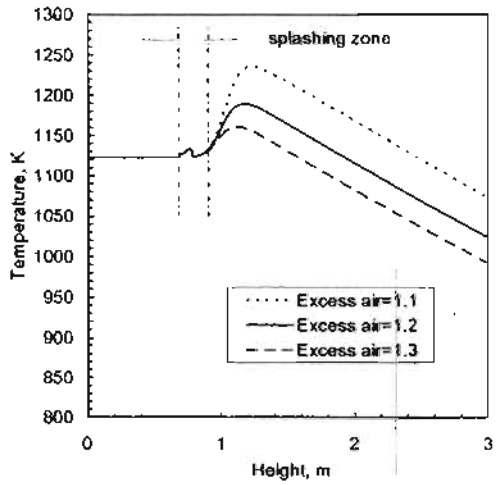

Fig. 9. Influence of excess air factor on axial temperature profile

Table 3 reports the influences of excess air factor on some important model outputs. In line with the trends discussed above the fraction of volatiles burns in the bed and the percentage of the heat released inside increase with the excess air factor. The heat recovered by ejected sand particles back to the bed increases with excess air factor as a smaller amount of unburned hydrocarbon burns past the splashing zone. The combustion efficiency always very high; however, it slightly improves with excess air factor mainly due to the lower concentration of exhausted CO.

The carbon loads of both coarse and fine char in the bed reduce with excess air factor. This trend is directly attributed to the higher oxygen concentration in the emulsion phase as shown in figure 10. This latter intensifies char burning rate (see Eq. 13). The elutriation rate of fine char is also reduces with excess air.

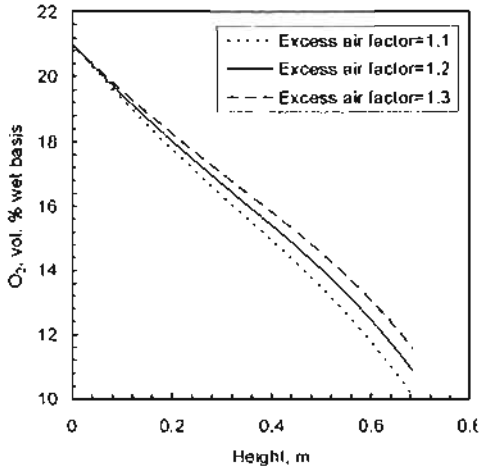

Fig. 10. Influence of excess air factor on axial concentration of O_2 in emulsion phase

Tab. 3. Influence of excess air factor on model results

		base case	
Excess air factor	1.1	1.2	1.3
Fraction of volatile burned within the bed, %	51.25	52.87	54.3
Fraction of heat release within the bed, %	60.47	61.77	62.94
Fraction of heat recovered by ejected sand, %	78.3	83.3	86.8
Average concentration of coarse char in the bed, kg/m^3	0.601	0.535	0.483
Average concentration of fine char in the bed, kg/m^3	.00316	0.00282	0.00255
Ratio of elutriated FC at the bed surface to fed fuel FC	3.92e-4	3.78e-4	3.67e-4
Maximum temperature in freeboard, K	1236	1189	1161
Max. overheating above bed temperature, °C	113	66	38
Maximum CH_4 concentration, %	4.61	4.11	3.7
Maximum CO concentration, %	0.86	0.823	0.785
Exhausted CO concentration, %	0.129	0.102	0.076
Ratio of exhausted FC from the combustor to fed fuel FC	1.47e-5	1.92e-6	2.94e-7
Combustion efficiency, %	99.5	99.59	99.67

4.2.2. Influence of bed temperature

The influences of bed temperature on combustion performance are estimated and presented in figures 11 and 12 in addition to table 4. As illustrated in figure 11a CH_y concentration in the bed zone grows with higher rates at lower bed temperature and then the peak concentration becomes more pronounced at the bed surface (see also table 4). Evidently the reaction rates lessen with decreasing bed temperature that allows a larger fraction of unburned hydrocarbon to surpass the bed (see table 4). For the same reason CO concentration still exhibits higher value at lower bed temperature as shown in figure 11b.

In the splashing zone the gas temperature is maintained close to the bed temperature for all cases considered in figure 12. The impact of temperature on the reaction rates is still almost the same as that in the bed. Therefore, larger fractions of CH_y and CO escape the splashing zone without combustion at lower bed temperature as shown in figure 11.a and 11.b, respectively. Shortly past the splashing zone there are dramatic changes in the profiles of CH_y, CO and gas temperature in the case of the lowest bed temperature (Tb=1073 K). CH_y and CO concentrations suddenly drop while there is a quasi instantaneous jump in gas temperature. Beyond the splashing zone the mutual effects between reaction rates and gas temperature appear very sensitive as the impact of ejected sand particles turns out to be insignificant. This mutual effect becomes more pronounced when larger fraction of combustible surpasses the splashing zone, more specifically at Tb=1073. The impact of operating bed temperature on freeboard overheating is major as depicted in figure 12. The overheating above bed temperature is predicted as 236, 66 and 8 K for operating bed temperature 1073, 1123 and 1173 K, respectively (see table 4). Thanks to this great overheating in freeboard CO concentration turns out to be very low at the combustor exit, about 30 ppm (see table 4).

As reported in table 4 the fraction of heat released in the bed increases with bed temperature as a higher amount of hydrocarbon burns in. Moreover, the heat recovery back to the bed by means of ejected sand particles becomes greater at the higher bed temperature since a smaller fraction of combustible burns past the splashing zone. It appears reasonable that combustion efficiency improves with bed temperature due to enhancement of combustion processes in bed and splashing zone as reported in table 4. The combustion efficiency; however, improves with decreasing bed temperature on the other side. This latter result should be mainly attributed to the high increase in gas temperature within freeboard that greatly minimizes the exhausted CO.

Table 4. Influence of bed temperature on model results

		base case	
Bed temperature, K	1073	1123	1173
Fraction of volatile burned within the bed, %	42.58	52.87	61.88
Fraction of heat release within the bed, %	53.4	61.77	69.1
Fraction of heat recovered by ejected sand, %	70.7	83.3	91.7
Average concentration of coarse char in the bed, kg/m^3	0.541	0.535	0.529
Average concentration of fine char in the bed, kg/m^3	.00288	0.00282	0.00276
Ratio of elutriated FC at the bed surface to fed fuel FC	3.59e-4	3.78e-4	3.96e-4
Maximum temperature in freeboard, K	1299	1189	1181
Max. overheating above bed temperature, °C	226	66	8
Maximum CH_y concentration, %	5.02	4.11	3.31
Maximum CO concentration, %	0.903	0.823	0.742
Exhausted CO concentration, %	0.003	0.102	0.04
Ratio of exhausted FC from the combustor to fed fuel FC	2.4e-6	1.92e-6	1.95e-6
Combustion efficiency, %	99.98	99.59	99.85

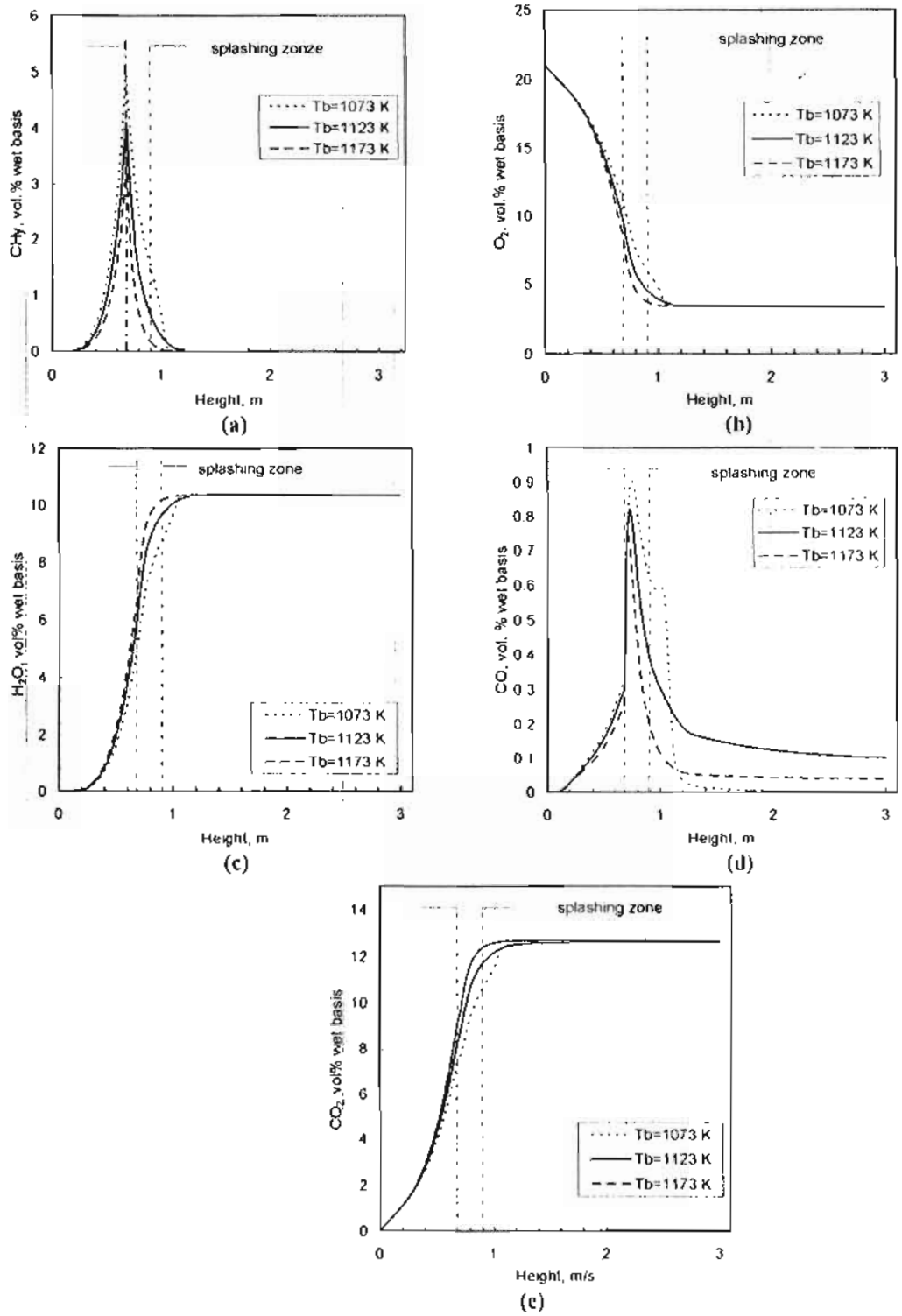

Figure 11. Influence of bed temperature on species concentration profiles

The influence of bed temperature on the bed carbon load is also reported in table 4. The average concentrations of coarse and fine chars reduce with increasing bed temperature due to enhancement of combustion kinetics. The elutriation rate of fine chars at the bed surface; however, slightly increases with bed temperature most likely because of viscosity effect. Alternatively, at the combustor exit the elutriated fine char is estimated to be the greatest in the case of the lowest bed

temperature even though freeboard exhibits the highest temperature as shown in figure 12. Obviously the higher gas temperature results in a higher gas velocity and in a shorter residence time. It appears that the impact of residence time on the fine char burning in freeboard overcomes the enhancement due to gas temperature.

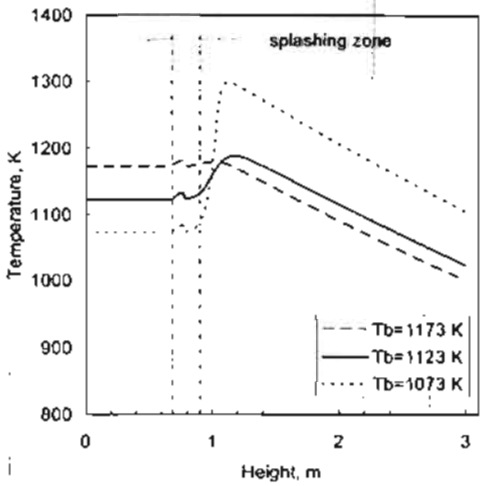

Fig. 12. Influence of bed temperature on axial temperature profile

4.2.3. Influence of fluidization velocity

Figures 13 and 14 as well as table 5 present the influences of fluidization velocity on combustion performance. The obtained results indicate that the peak value of CH_y concentration becomes higher with increasing fluidization velocity (see figure 13.a & table 5). This result appears realistic as gas residence time decreases with increasing fluidization velocity. Thus greater fraction of unburned hydrocarbon reaches splashing zone resulting in more intensive combustion processes inside. As a consequence the peak of CO concentration becomes more pronounced with increasing fluidization velocity as shown in figure 13.b and the maximum value of CO concentration turns out to be greater as reported in table 5. It is also noted that the peak position and the splashing zone are shifted up as the bed expands higher with fluidization velocity.

The influence of fluidization velocity on temperature profile is shown in figure 14. Differently from the above results the first smaller temperature peak in the splashing zone notably gets higher with increasing fluidization velocity. The first peak temperature values are predicted 1129, 1133 and 1146 K corresponding to fluidization velocities 0.75, 1 and 1.25 m/s, respectively. This result is attributed to multiplying heat release rate in the splashing zone mainly due to increasing fuel feed rate to keep constant excess air factor. The greater fraction of unburned hydrocarbon that reaches the splashing zone at higher fluidization velocity gives a further contribution. In freeboard beyond the splashing zone the maximum temperature gets higher with increasing fluidization velocity because a larger fraction of combustibles surpass the splashing zone. The maximum overheating in freeboard above the bed temperature is reported in table 5 as a function of fluidization velocity.

In accordance with the above results the fraction of heat released in the bed reduces with increasing fluidization velocity as reported in table 5. The recovered heat by ejected sand particles decreases with fluidization velocity as larger fractions of combustibles surpass splashing zone. Combustion efficiency slightly changes according to the exhausted CO concentration. The coarse and fine concentrations in the bed slightly vary with non-monotonic trend because three factors mainly affect their value with different impact. Oxygen concentration in emulsion phase which increases with fluidization velocity as depicted in figure 15. Of course the higher O_2 concentration reduces char concentration. The second factor is the feed rate of original char that increases with increasing fluidization velocity since excess air factor is kept constant. It should increases char concentration. The last parameter is the expanded bed height that grows with fluidization velocity. This latter should lessen the char concentrations. The elutriation rate increases slightly with fluidization velocity.

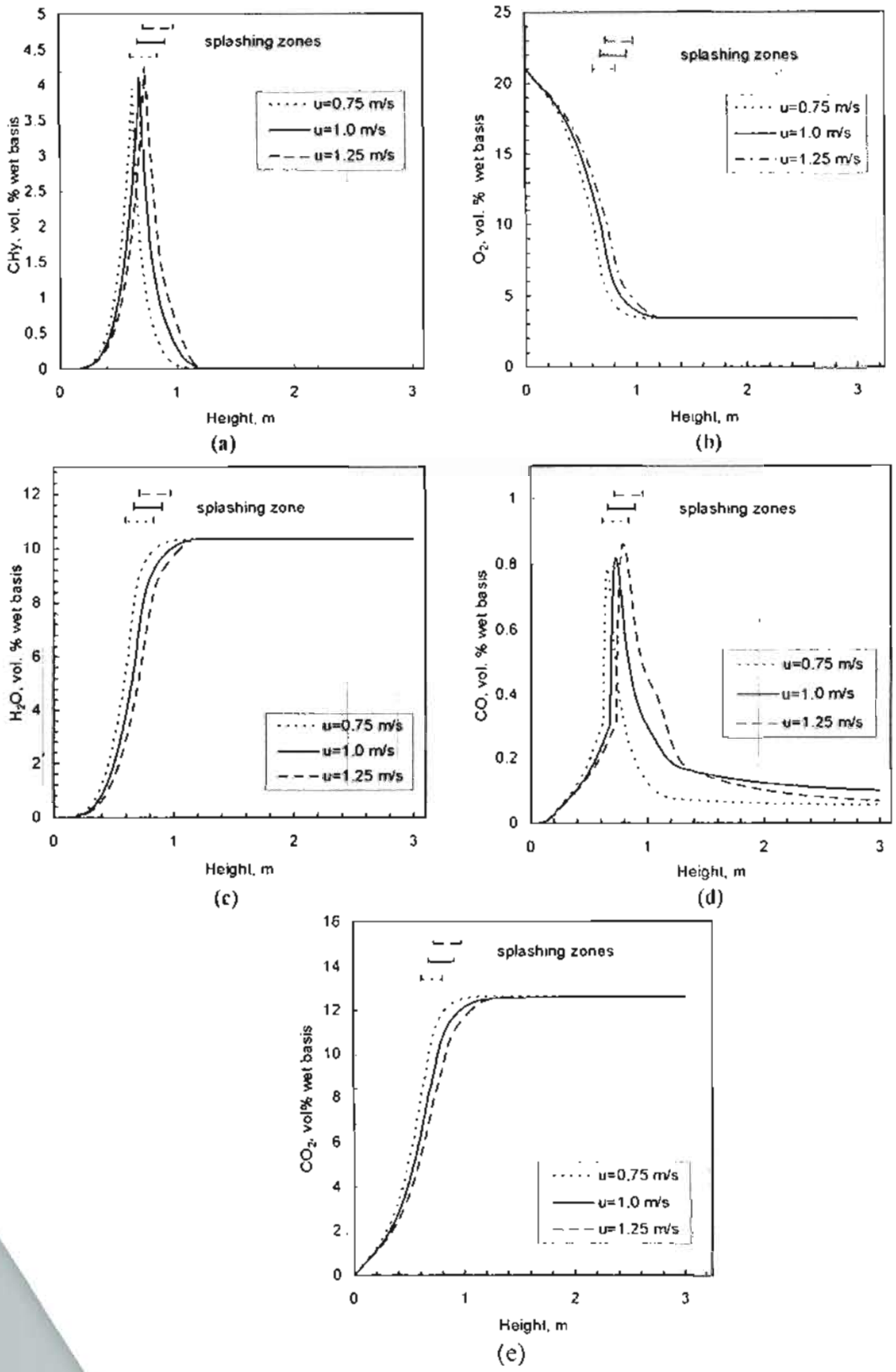

Fig. 13. Influence of fluidization velocity on species concentration profiles

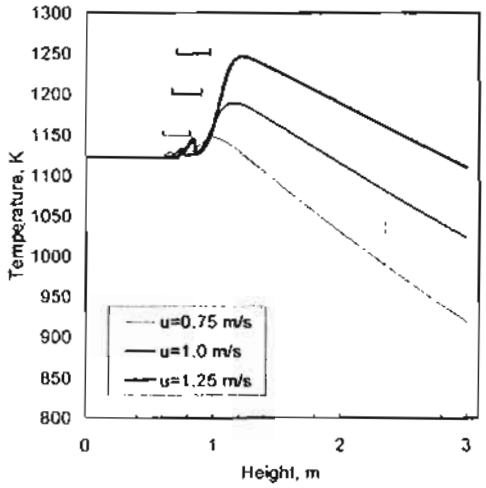

Fig. 14. Influence of fluidization velocity on axial temperature profile

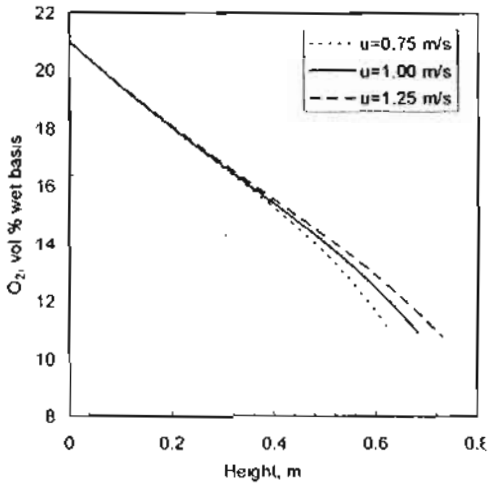

Fig. 15. Influence of fluidization velocity on axial concentration of O_2 in emulsion phase

Tab. 5. Influence of fluidization velocity on model results

		base case	
Fluidization velocity, m/s	0.75	1.0	1.25
Fraction of volatile burned within the bed, %	54.47	52.87	51.13
Fraction of heat release within the bed, %	63.07	61.77	60.37
Fraction of heat recovered by ejected sand, %	88.34	83.3	77.94
Average concentration of coarse char in the bed, kg/m^3	0.433	0.535	0.53
Average concentration of fine char in the bed, kg/m^3	0.0023	0.00282	0.00275
Fraction of elutriated FC at the bed surface to fed fuel FC	2.29e-4	3.78e-4	4.62e-4
Maximum temperature in freeboard, K	1147	1189	1246
Max. overheating above bed temperature, °C	24	66	123
Maximum CH_y concentration, %	3.96	4.11	4.26
Maximum CO concentration, %	0.789	0.823	0.861
Exhausted CO concentration, %	0.057	0.102	0.068
Fraction of exhausted FC from the combustor to fed fuel FC	1.37e-6	1.92e-6	2.22e-6
Combustion efficiency, %	99.77	99.59	99.70

5. CONCLUSIONS

A one-dimensional model has been presented to simulate fluidized bed combustion of straw-bitumen-pellets based on the two-phase theory of fluidization. The model considers and simplifies the different important processes including volatile release and segregation, char comminution and elutriation, bed particles ejection and post-combustion in splashing zone and freeboard. Although the model is rather simplified it describes in a good way the combustion performance and the influence of operating variables. The model yields the axial profiles of different species concentrations in the two bed phases (bubble and emulsion), in the splashing zone and in the freeboard. In particular, the model predicts the axial temperature profile in the splashing and freeboard zones.

The model results estimate that about 53% of volatiles combustion and 62% of the total heat release take place within th
considering the basis case co
fraction of heat release
zone is about 33
portion (7%
the splas
particles
about
zone.

tempera
maximu
the splas

overheating as the ejected sand particles recover the great part of released heat. The second maximum arises in the freeboard where the flux of the ejected particles turns out to be very few and its impact on gas temperature becomes insignificant. The second maximum is relatively much higher with 66 °C overheating.

Combustion efficiency is always very high, greater than 99.5%. Char concentration in the bed is estimated to increase with height that appears more realistic than uniform concentration. It is based on the assumption that the fresh fed char is uniformly distributed along the bed height. The rate of elutriated fine char is very low.

The influences of operating variables on the combustion performance have been evaluated. The fractions of volatile burning and heat release within the bed; and the fraction of heat recovered by ejected sand particles are found to increase with increasing excess air factor, with increasing bed temperature and with decreasing fluidization velocity. Alternatively the maximum overheating temperature in freeboard becomes higher with decreasing excess air factor, with lowing bed temperature and with increasing fluidization velocity. Bed temperature among the others has the highest impact on combustion performance.

An acceptable agreement are found between the predicted and the measured concentrations and temperature profiles.

REFERENCES

1. Achara N., Horsley M. E., Purvis M. R. I., and Teague R. H. (1984) "The combustion of palletized refuse derived fuel in fluidized beds" In Proc. of the third international Fluidized conf. London: The Institute of Energy, DISC/25/215.
2. Adánez J., de Diego L.F., Garcia-Labiano F., Abad A. and Abánades J.C. (2001) "Determination of Biomass Char Combustion Reactivities" In Proc. of the 16th international conf. on FBC, FBC01-0111, Reno Nevada. ASME.
3. Adanez J. de Diego L. F. Gayan P. Garcia-Labiano F Cabanillas A. and Bahillo A. (2003) "Co-combustion of biomass and coal in circulating fluidized bed: modeling and validation" Proc. 17th International Conf. on FBC, p. FBC2003-064, Florida, ASME.
4. Amand L., Miettinen-Westberg H., Karlsson M., Leckner B., Luecke K., Budinger S., Hartge E.U., and Werther J. (2001) "Co-combustion of dried sewage sludge and coal/wood in CFB. A search for factors influencing emissions" Proc. 16th Intern. Conf. on FBC, New York.
5. Andersson B. A., Leckner B., and Amand L. E. (1985) "Fluidized bed combustion of coals and alternative fuels" In Proc. of 8th international conf. on FBC, pp. 1019–1029, New York.
6. Arena U., D'Amore M. and Massimilla L. (1983) "Carbon attrition during the fluidized combustion of a coal" A.I.Ch.E. Journal, 29, 40.
7. Arena U., Cammarota A. and Chirone R. (1995a) "Fragmentation and attrition during the fluidized bed combustion of two waste-derived fuels" In J.-F. Large & C. Laguerie (Eds.) Fluidization VIII, pp. 437–444, New York: Engineering Foundation.
8. Arena U. Cammarota A. Chirone R. and D'Anna G. (1995b) "Comminution phenomena during the fluidized bed combustion of a commercial refuse-derived fuel" In Proc. of the 13th intern. conf. on FBC, pp. 943–949, New York.
9. Arena U., Chirone R., D'Amore M., Miccio M. and Salatino P. (1995c) "Some issues in modeling bubbling and circulating fluidized-bed combustors", Powder Technology 82 301.
10. Armesto L. Cabanillas A. Bahillo A. Segovia J.J. Escalada R. Martinez J.M. Carrasco J.E. (1997) "Coal and biomass co-combustion on fluidized bed: comparison of circulating and bubbling fluidized bed technologies" Proc. 14th

International Conf. on FBC, pp. 301-311, ASME, New York.

11. Atimtay A. T. (1980) "Combustion of volatile matter in fluidized beds" In J. R. Grace & J. M. Matsen (Eds.) Fluidization, pp. 159–166, New York: Plenum.
12. Baron T., Briens C. L., Galtier P. and Bergougnou M. A. (1990) "Effect of bed height on particle entrainment from gas-fuldized beds" Powder Tech. J, 63, 149.
13. Benoni D., Briens C. L., Baron T., Duchesne E. and Knowlton T. M. (1994) "A procedure to determine particle agglomeration in a Fluidized Bed and its effect on entrainment" Powder Technology, 78, 33.
14. Borodulya V. A., Didalenko V. I., Palchonok G. I. and Stanchitis L. K. (1995) "Fluidized bed combustion of solid organic wastes and low-grade coals: research and modeling" In Proc. of the 13th international conf. on FBC, pp. 935–942, New York: ASME.
15. Briens C. L, Bergougnou M. A. and Baron T. (1988) "Prediction of entrainment from gas-golid fluidized beds" Powder Technology, 54, 183.
16. Chirone R., D'Amore M., Massimilla L. and Salatino P. (1984) "The efficiency of fluidized combustion of carbons of various characteristics" In Proc. of the conference: combustion of tomorrow's fuels- II (pp. 313–335), New York: Engineering Foundation.
17. Chirone R., Marzocchella A., Salatino P. and Scala F.(1999) "Fluidized bed combustion of high-volatile solid fuels: an assessment of char attrition and volatile matter segregation" In Proc. of the 15th international conf. on FBC, FBC01-0111, Savannah, ASME.
18. Darton R. C., La Nauze R. D., Davidson J. F. and Harrison D. (1977) "Bubble growth due to coalescence in fluidized beds" Transactions of the Institution of Chem. Eng., 55, 274.
19. Davidson J. F. (1992) "Rapporteur's review of the papers dealing with fundamental aspects of Fluidization and emission science" Journal of the Institute of Energy, 65, 2.
20. Ekmann J.M., Smouse S.M., Wilnslow J.C., Ramezan M. and Harding N.S. (1996), "Co-firing of coal and wastes" IEACR/90, IEA Coal Research.
21. Fahlstedt I., Lindberg T., Lindman E. and Anderson J. (1997) "Co-firing of biomass and coal in a pressurized fluidized bed combined cycle. Results of pilot plant studies", Proc. 14th Intern. Conf. on FBC, pp. 295-300, New York.
22. Faravelli T., Frassoldati A., Ranzi A., Miccio F. and Miccio M (2003) "Modeling homogeneous combustion in bubbling beds burning liquid fuel", Proc. of 17th Int. FBC Conf., paper 133,ASME.
23. Faravelli T., Frassoldati A., Ranzi A., Miccio F. and Miccio M (2004) "Modeling hydrocarbon oxidation and pollutant formation in FBC of liquid fuels" Proc. of the 11th int. Conf. On Fluidization, EE4, Naples, Italy.
24. Fiorentino M., Marzocchella A. and Salatino P. (1997a) "Segregation of fuel particles and volatile matter during devolatilization in a fluidized bed reactor-I. Model development" Chemical Engineering Science, 52, 1893.
25. Fiorentino M., Marzocchella A. and Salatino P. (1997b) "Segregation of fuel particles and volatile matter during devolatilization in a Fluidized bed reactor-II. Experimental", Chemical Engineering Science, 52, 1909.
26. Fung A. S., and Hamdullahpur F. (1993) "Effect of bubble coalescence on entrainment in gas fluidized beds", Powder Technology, 77, 251.
27. George S. E. and Grace J. R. (1978) "Entrainment of particles from aggregative Fluidized beds", A.I.Ch.E. Symposium Series (176), 74, 67.
28. Gulyurtlu I. and Cabrita I. (1984) "Fluidized bed combustion of forestry wastes and low-quality coals" In Proc. of the third intern. Fluidized conf. London: The Institute of Energy. DISC/11/80.
29. Gulyurtlu I., Reforco A. and Cabrita I. (1991) "Fluidized combustion of

corkwaste", In Proc. of the 11th international conf. on FBC, pp. 1421-1424, New York, ASME.

30. Hampartsoumian E. and Gibbs B. M. (1980) "Combustion of peat in a fluidized bed", Institute of Energy Symposium Series 4, IIB–3-1.
31. Hein K.R.G. and Bemtgen J.M. (1998) "EU clean coal technology- co-combustion of coal and biomass", Fuel Proc. Tech. 54, pp. 159-169.
32. Hayurst A.N. and Tucker R.F. (1990) "The combustion of carbon monoxide in a two zone fluidized bed" Combustion and Flame, Vol. 79, pp.175-189.
33. Hilligardt and Werther J. in Proc. 3rd World Cong. Of Chem. Eng. Tokyo (1986). Werther J. in Fluidization IV Kunni D. and Toei R. p. 93 Eng. Foundation 1983 New York.
34. Irusta R. Antolin G. Velasco E. and De Miguel R. (1995) "Modelling of lignocellulose waste combustion in an atmospheric bubbling fluidized bed using an internal devolatilization degree parameter", In J.-F. Large & C. Laguerie (Eds.) Fluidization VIII, pp. 855–862. New York: Engineering Foundation.
35. Jovanovic L. and Oka S. (1984) "Fluidized bed combustion of low grade fuels", In Proc. of the conf.: combustion of tomorrow's fuels-II (pp. 351–359). New York: Eng. Foundation.
36. Kakaras E., Vourliotis P., Grammelis P. (2001) "Co-combustion of lignite with waste wood in a lab-scale fluidized bed" Proc. 16th Internat. Conf. on FBC, New York, ASME.
37. Kunii D. and Levenspiel O. (1991) "Fluidization Engineering" Butterworth-Heinemann Second Edition.
38. Leckner B., Andersson B. A. and Vijil J. (1984) "Fluidized Bed Combustion of Coal and Biomass" In Proc. of the conf.: combustion of tomorrow's fuels-II, pp. 401–410. New York: Engineering Foundation.
39. Leckner B., Palchonok G.I. and Andersson B. A. (1992), "Representation of heat and mass transfer of active particles" Presented at the IEA-FBC, Mathematical Modelling Meeting, Turku, Finland.
40. Leckner B. and Karlsson M. (1993) "Emissions from circulating fluidized bed combustion of mixtures of wood and coal", in Proc. 12th International Conf. on FBC, p. 109-115, Press New York.
41. Loeffler G. and Hofbauer H. (2002). "Does CO burn in a fluidized bed?-A detailed chemical kinetic modeling study" Comb. and Flame, Vol. 129, pp.439-452.
42. Madrali E. S., Ercikan D. and Ekinci E. (1991) "Changes in fuel particle structure and its effect on segregation in fluidized beds during the initial combustion stages" In FBC technology and the environmental challenge, pp. 139–147, Bristol: Hilger.
43. Miccio F., Miccio M., and Olivieri(2001) G. " A study on Bubbling Bed Combustion of Gasoil", In Proc. of the 16th International Conference on FBC, FBC01-0178, Reno, USA.
44. Miccio F., Scala F. and Chirone R. (2003) "FB combustion of a biomass fuel: comparison between pilot scale experiments and model simulations", In Proc. of 17th International Conf. on FBC, FBC2003-033, Florida, USA.
45. Miccio F and Okasha F. (2004), "Fluidized Bed Combustion and Desulfurization of a Heavy Liquid Fuel" Chemical Engineering Journal (Elsevier), Vol. 105/3, pp 81-89.
46. Milioli F. E. and Foster P. J. (1995) "Entrainment and elutriation modeling in bubbling fluidized beds" Powder Technology, 83, 233.
47. Ogada T. (1995) "Emissions and combustion characteristics of wet sewage sludge in a bubbling fluidized bed"' PhD Thesis, Tech. Univ. of Hamburg-Harburg.
48. Okasha F., El-Emam S. H., and Mostafa H. K (2003) "The fluidized bed combustion of heavy liquid fuel (mazut)", Experimental Thermal and Fluid Science, 27, 4, pp. 473-480.
49. Okasha F. and Miccio M. (2006) "Modeling of wet jet in fluidized bed",

Chemical Engineering Science, Vol. 61, Issue 10, pp. 3079-3090

50. Okasha F., Cammarota A., Urciuolo M. and Chirone R. (2006) "Combustion of combined rice straw-bitumen-pellets in fluidized bed" 19th International Conference on FBC, May, Vienna.
51. Okasha F. (2006) "Modeling of liquid fuel combustion in fluidized bed" submitted to Mansoura Eng. Journal.
52. Peel R. B. and Santos F. J. (1980) "Fluidized bed combustion of vegetable fuels" Institute of Energy Symposium Series, 4, IIB-2.
53. Park D., Levenspiel O. and Fitzgerald T. J. (1980) "A Plume model for large scale atmospheric fluidized bed combustors" In Proc. of the sixth intern. conf. on FBC, pp. 791–802. New York: ASME.
54. Park D., Levenspiel O. and Fitzgerald T. J. (1981) "Plume model for large particle fluidized-bed combustors", Fuel, 60, 295.
55. Pemberton S. T. and Davidson J. F. (1984) "Turbulence in the freeboard of a gas-fluidized bed-the significance of ghost bubbles" Chem. Eng. Sci., 39, 829.
56. Pemberton S. T. and Davidson J. F. (1986) "Elutriation from fluidized beds-I. Particle ejection from the dense phase into the freeboard" Chemical Engineering Science, 41, 243.
57. Philippek C., Knobig T, Schnfelder H. and Werther J. (1997) "NOx formation and reduction during combustion of wet sewage sludge in the circulating fluidized bed-measurement and simulation", 14th International Conference on FBC.
58. Pillai K. K. (1981) "The influence of coal type on devolatilization and combustion in Fluidized beds" Journal of the Institute of Energy, 54, 142.
59. Prins W. (1987) "Fluidized bed combustion of a single carbon particle" Ph.D. Thesis, University of Twente, The Netherlands.
60. Salatino P., Scala F., Chirone R. and Pollesel P. (1997) "Optimization by air staging of the fluidized bed combustion of tyre derived fuel" In Proc. of the 4th international Conf. on technologies and combustion for clean environment, pp. 23–27, Portugal, Lisbon.
61. Salatino P., Scala F. and Chirone R. (1998) "Fluidized bed combustion of a biomass char: the influence of carbon attrition and fines post-combustion on fixed carbon conversion" Proceedings of the Combustion Institute, 27, 3103.
62. Scala and Salatino (2002) "Modelling fluidized bed combustion of high-volatile solid fuels" Chemical Engineering Science, vol. 57, pp. 1175-1196.
63. Scala F. (1998) "Fluidized Bed Combustion of High-Volatile Solid Fuels" Ph.D. thesis Universita degli Studi di Napoli Federico II, Naples, Italy.
64. Selcuk N., Degirmenci E, Gogebaken (2001) "Modeling of a bubbling AFBC with volatiles release" In Proc. 16th International Conf. on FBC, New York.
65. Stubington J. F. and Davidson J. F. (1981) "Gas-Phase Combustion in Fluidized Beds" A.I.Ch.E. Journal, 27, 59.
66. Stubington J. F., Chan S. W. and Clough S. J. (1990) "A model for volatiles release into bubbling fluidized bed combustor" A.I.Ch.E. Journal, 36, 7585.
67. Stubington J. F. and Chan S. W. (1993) "The multiple discrete diffusion flame model for fluidized bed combustion of volatiles" In Proc. of the 12th international conference on fluidized bed combustion, p. 167. New York: ASME.
68. Van der Honing G. (1991) "Volatile and char combustion in large scale Fluidized bed coal combustors" Ph.D. thesis University of Twente, The Netherlands.
69. Werther J., Hartge E.U., Luecke K., Fehr M., Amand L.E. and Leckner B. (2000) "New air-staging techniques for co-combustion in fluidized bed combustors" VGB-Conference Research for power plant technology, p. 1-12.
70. Yates J. G., Macgillivray M. and Cheesman D. J. (1980) "Coal devolatilization in fluidized bed combustors", Chem. Eng. Sc. J, 35, 2360.